Van der Waals epitaxy of functional MoO_2 film on mica for flexible electronics

Chun-Hao Ma, Jheng-Cyuan Lin, Heng-Jui Liu, Thi Hien Do, Yuan-Min Zhu, Thai Duy Ha, Qian Zhan, Jenh-Yih Juang, Qing He, Elke Arenholz, Po-Wen Chiu' , and Ying-Hao Chu'

Citation: Appl. Phys. Lett. **108**, 253104 (2016); doi: 10.1063/1.4954172
View online: http://dx.doi.org/10.1063/1.4954172
View Table of Contents: http://aip.scitation.org/toc/apl/108/25
Published by the American Institute of Physics

Articles you may be interested in

Van der Waals epitaxy of ultrathin α-MoO3 sheets on mica substrate with single-unit-cell thickness
Appl. Phys. Lett. **108**, 053107053107 (2016); 10.1063/1.4941402

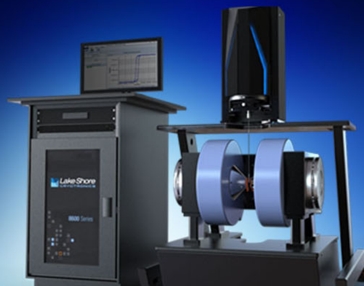

APPLIED PHYSICS LETTERS 108, 253104 (2016)

Van der Waals epitaxy of functional MoO_2 film on mica for flexible electronics

Chun-Hao Ma,[1,2] Jheng-Cyuan Lin,[3] Heng-Jui Liu,[2] Thi Hien Do,[2] Yuan-Min Zhu,[4] Thai Duy Ha,[5] Qian Zhan,[4] Jenh-Yih Juang,[5] Qing He,[6] Elke Arenholz,[7] Po-Wen Chiu,[1,8,a)] and Ying-Hao Chu[2,3,5,b)]
[1]Department of Electrical Engineering, National Tsing Hua University, 30013 Hsinchu, Taiwan
[2]Department of Materials Science and Engineering, National Chiao Tung University, Hsinchu 30010, Taiwan
[3]Institute of Physics, Academia Sinica, Taipei 11529, Taiwan
[4]School of Materials Science and Engineering, University of Science and Technology Beijing, Beijing 100083, China
[5]Department of Electrophysics, National Chiao Tung University, Hsinchu 30010, Taiwan
[6]Department of Physics, Durham University, Durham DH1 3LE, United Kingdom
[7]Advanced Light Source, Lawrence Berkeley National Laboratory, Berkeley, California 94720, USA
[8]Institute of Atomic and Molecular Sciences, Academia Sinica, Taipei 10617, Taiwan

(Received 25 March 2016; accepted 5 June 2016; published online 20 June 2016)

Flexible electronics have a great potential to impact consumer electronics and with that our daily life. Currently, no direct growth of epitaxial functional oxides on commercially available flexible substrates is possible. In this study, in order to address this challenge, muscovite, a common layered oxide, is used as a flexible substrate that is chemically similar to typical functional oxides. We fabricated epitaxial MoO_2 films on muscovite via pulsed laser deposition technique. A combination of X-ray diffraction and transmission electron microscopy confirms van der Waals epitaxy of the heterostructures. The electrical transport properties of MoO_2 films are similar to those of the bulk. Flexible or free-standing MoO_2 thin film can be obtained and serve as a template to integrate additional functional oxide layers. Our study demonstrates a remarkable concept to create flexible electronics based on functional oxides. *Published by AIP Publishing.*
[http://dx.doi.org/10.1063/1.4954172]

To achieve low-power consumption, multifunctional, and environmentally friendly electronics, functional materials have to meet more requirements. For example, instead of having functional systems and electronic circuits on rigid substrates, "flexible electronics," i.e., integrated circuits that are built on bendable materials or freestanding without any support, represents a rapidly developing field that has a great potential to impact our daily life.[1–3] To develop flexible electronics, materials with controllable conduction and suitable mechanical properties, i.e., robustness against cracking, are required.[4–6] Recently, the discovery of free-standing 2D materials has revolutionized this field.[7–9] Like graphene, these 2D materials exhibit many unusual physical phenomena that are not found in the bulk. For example, the electronic band structure of graphene has a linear dispersion near the K points and, accordingly, the charge carriers should be massless, suggesting ultra-high electron mobility.[10–12] Moreover, it is nearly transparent in the visible spectral range.[13–15] Superior charge and heat transport in such 2D system offer possibilities for device development. However, the extensively studied pristine graphene has no bandgap, which limits the applications based on field-effects. Hence, identifying promising 2D materials is an important research direction.[16,17] A good example is the resurgence of scientific and engineering interests in transition metal dichalcogenides,[18–20] which exhibit the diverse properties ranging from semiconducting and metallic to superconducting (e.g., MoS_2, $NbSe_2$, etc.). While this research direction keeps expanding, it is worth addressing an important question that whether the existing and well-studied material systems can be integrated into flexible electronics.

The interplay of electronics, spin, orbital, and lattice degrees of freedom in functional oxides create a rich spectrum of competing phases and intriguing physical properties.[21] Recently, many studies have suggested that oxide heterostructures provide a powerful route to manipulate these degrees of freedom and offer possibilities for next-generation functional devices.[22,23] However, a method to fabricate flexible electronics incorporating functional oxides is yet to be developed. Van der Waals epitaxy[24–26] makes use of an epitaxial relationship among different materials and weak interfacial van der Waals bonds. Van der Waals epitaxy has been applied to the epitaxial growth of various material systems. For example, 2D materials can be deposited epitaxially on 3D materials such as Sapphire[27–29] and then easily removed from the substrate and transferred onto other materials for device fabrication. Moreover, this approach has been utilized to create free standing films of 3D materials: The 3D materials are grown in thin film form on a 2D material and the two materials are then separated.[30–34] In the present study, we employ this same concept to provide a route for the development of flexible electronics based on functional oxides. Muscovite, a type of mica, is a layered oxide. Due to the weak interlayer van der Waals force, atomically flat (001) surfaces can be created by exfoliation along the (001) plane, making it a suitable substrate for van der Waals epitaxy.[35] Moreover, muscovite is transparent and flexible when its thickness is in the micrometer range and with that muscovite is suitable for flexible and

a)Electronic mail: pwchiu@ee.nthu.edu.tw
b)Electronic mail: yhc@nctu.edu.tw

transparent electronics if integrated functional devices can be implemented on it. The key challenge is to deposit a 3D functional oxide epitaxially on 2D layered muscovite. Devices made of epitaxial material systems typically show a better performance compared with amorphous or polycrystalline.[36,37] In order to obtain high performance devices based on functional oxides deposited on muscovite substrates for flexible electronics, a good metallic layer for electrical contacts is necessary. MoO_2 has high conductivity and also provides a suitable base layer for heteroepitaxy of other functional oxides. In this manuscript, we demonstrate the integration of 3D functional MoO_2 on muscovite as a model system. Van der Waals epitaxy of MoO_2 films on muscovite is studied by a combination of *in-situ* reflective high energy electron diffraction (RHEED), XRD, and transmission electron microscopy (TEM) measurements. To demonstrate its functionalities, a p-type metallic system is realized in the MoO_2/muscovite heterostructure. Flexible MoO_2 films on muscovite or free-standing MoO_2 thin films can be fabricated by this approach. Our results represent an important step to establish flexible electronics based on the conventional 3D functional oxides.

Van der Waals epitaxial MoO_2 thin films were grown on a (001) native muscovite substrate by pulsed laser deposition (PLD), using a KrF excimer laser ($\lambda = 248$ nm, Lambda Physik) operated at 10 Hz repetition rate and 200 mJ output laser power. In order to obtain pure MoO_2 phase, the deposition was carried out in the oxygen pressure range of $\sim 10^{-6}$ Torr with the substrate temperature of 400 °C. Pure MoO_3 phase can also be acquired when an oxygen pressure higher than 10^{-2} Torr was used. In the pressure range of 10^{-4} to 10^{-2} Torr, a mixture of MoO_2 and MoO_3 could be generated. Reflective high-energy electron diffraction was used to monitor the growth mode on the sample surface during the growth process. High-resolution X-ray diffraction experiments were performed at the BL17A at the National Synchrotron Radiation Research Center in Hsinchu. Cross-sectional samples for TEM studies were prepared by a standard ion milling technique. Microstructural investigations were done on a FEI Tecnai G^2 F20 with an information limit of 1.4 Å. Chemical composition analysis was achieved by electron spectroscopy. X-ray photoelectron spectroscopy (XPS) spectra were obtained by ULVAC-PHI PHI 5000 Versaprobe II. The electrical characterization was performed in a physical properties measurement system (Quantum Design).

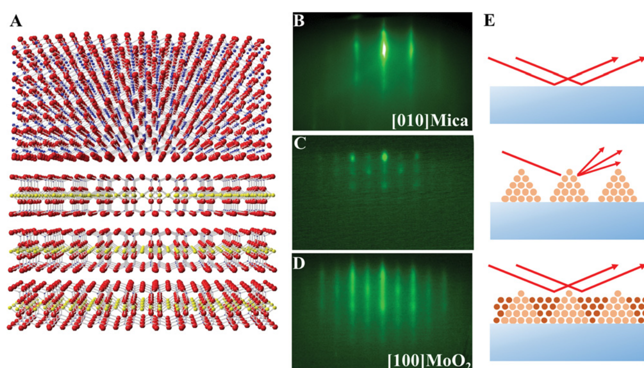

FIG. 1. (a) Schematic representation of van der Waals epitaxial MoO_2 (top, Mo in blue and O in red) on muscovite (bottom, Si in yellow and O in red). RHEED patterns recorded (b) before the deposition, (c) in the early stage of growth, and (d) after the deposition process. (e) Schematic of growth mechanism.

In this study, epitaxial MoO_2 thin films (Figure 1(a)) were grown on (001) native muscovite by pulsed laser deposition (PLD). *In-situ* RHEED was employed to investigate the growth mode during the deposition. Before the deposition, a typical RHEED pattern of the cleaved muscovite substrate was recorded along the [010] crystal orientation as shown in Figure 1(b). The image shows strong Laue diffraction spots and an array of vertical straight streaks, indicating that the cleaved surface is nearly atomically smooth which we also confirmed by atomic force microscopy. When the deposition of MoO_2 begins, the RHEED pattern of the muscovite substrate disappears rapidly and a spot-like pattern (Figure 1(c)) emerges indicative of an island growth mode of the epitaxial MoO_2. Analyzing the RHEED pattern carefully, by calculating the distances between the diffraction spots, we can easily identify that the MoO_2 $\langle 001 \rangle$ direction is aligned parallel with muscovite $\langle 100 \rangle$ direction. Interestingly, as the deposition continues, a quasi-2D pattern re-emerges, which is reflected by the diffraction spots becoming weak and gradually transforming into vertical straight streaks (Figure 1(d)), an indication of the formation of a smooth surface and high crystalline quality of the deposited MoO_2 thin film. The growth mechanism is illustrated in Figure 1(e). The ablated MoO_2 clusters initially favor the formation of nanocrystals because of their weak bonding (van der Waals force) to the muscovite substrate. However, the structural similarities between MoO_2 and muscovite substrate (both are monoclinic oxides) favor epitaxial growth. When more clusters accumulate on the substrate, these nanocrystals prefer to grow in lateral direction and then merge together to form a continuous film.

The structural characteristics were further examined by high-resolution X-ray diffraction. Figure 2(a) shows a typical out-of-plane θ-2θ scan of the MoO_2/muscovite heterostructure. Only muscovite (00L) and MoO_2 (0K0) diffraction peaks can be detected, indicating high crystalline quality of thin film without secondary phases. In addition, it clearly confirms the crystalline orientation derived from the RHEED pattern to be $\langle 010 \rangle$ $MoO_2 || \langle 001 \rangle$ muscovite. The lattice constant of MoO_2 determined from the XRD result is 4.87 Å, which is very close to the bulk value. Thus, the film is almost fully relaxed as expected for van der Waals epitaxy. Furthermore, Φ-scans of the MoO_2 (022) and muscovite (202) reflections were used to determine the in-plane structural relationship, as shown in Figure 2(b). The muscovite (202) plane originally presents a two-fold symmetry due to its monoclinic tilting angle between a- and c- axes ($\beta = 100°$). Therefore, the observation of three muscovite (202) peaks at 120° intervals indicates that there are three different configurations corresponding to an alternating stacking sequence of muscovite.[38] A similar result can be observed in the MoO_2 (022) plane as well. Monoclinic MoO_2 has a two-fold symmetry, and therefore the presence of six peaks in the Φ-scan of the (022) plane at 60° intervals reveals the co-existence of three sets of domains in the MoO_2 thin film. The good alignment of muscovite (202) and MoO_2 (022) peaks at 0°, 120°, and 240° confirms the in-plane epitaxial relationship as $\langle 100 \rangle$ muscovite$|| \langle 001 \rangle$ MoO_2, in an excellent agreement with the RHEED results. Measurements of the rocking curve were conducted to obtain more information about the crystalline quality.

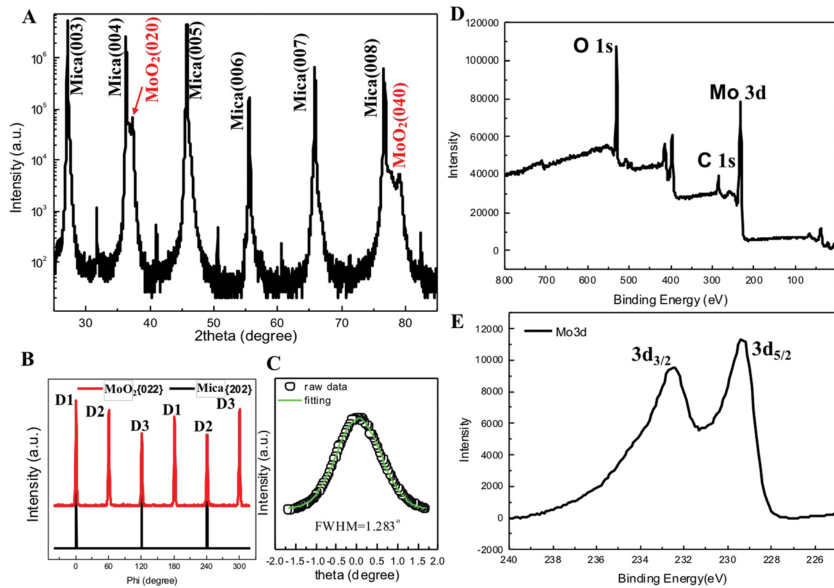

FIG. 2. (a) Out-of-plane X-ray diffraction of MoO_2 on muscovite. (b) Phi scan of MoO_2 {022} and muscovite {202}. (c) Rocking curve of MoO_2 (020). (d) Surface XPS spectrum of MoO_2/muscovite. (e) High-resolution spectrum of Mo 3d core level.

The full width at half maximum of the MoO_2 (020) feature is $\sim 1.3^\circ$ as shown in Figure 2(c). We have attempted to further improve the crystallinity by varying the growth conditions. In order to obtain higher quality MoO_2 films, control of domain structure is essential since the crystallinity of films is dominated by the multidomain structure.

In order to verify the valence state of Mo ions in the heterostructure and to confirm the chemical composition, we carried out X-ray photoelectron spectroscopy (XPS) measurements. Figure 2(d) shows a typical XPS spectrum obtained from the surface of the MoO_2 thin films. In the spectrum, only the peaks associated with Mo 3d, O 1s, and C 1s states were detected, confirming that no other elements are present in the film. Figure 2(e) shows a high resolution spectrum of the Mo 3d core levels, which is composed of a mixture of Mo $3d_{5/2}$ and $3d_{3/2}$ spin doublets in various oxidation states of Mo. The Mo^{4+} $3d_{5/2}$ peak at 229.3 eV and the Mo^{4+} $3d_{3/2}$ peak at 232.5 eV were detected with negligible intensities of the other peaks contributing from Mo^{5+} and Mo^{6+}, which ascertains the valence state of Mo to be +4 in the heterostructures.

In order to confirm the van der Waals epitaxy, we employed TEM to study the interface structure. In Figure 3(a), a low-magnification cross-sectional TEM image shows the flat interface of the MoO_2 film on muscovite. The corresponding electron diffraction patterns of an area near the interface between the MoO_2 thin film and muscovite substrate are shown in Figure 3(b). Reciprocal lattices of both MoO_2 and muscovite are clearly visible and the epitaxial relationship is $\langle 010 \rangle$ $MoO_2 || \langle 001 \rangle$ muscovite and $\langle 001 \rangle$ $MoO_2 || \langle 100 \rangle$ muscovite. This result is consistent with the conclusions made from the RHEED and XRD analyses. Figure 3(c) shows a high-resolution TEM (HR-TEM) image of the interface as marked in Figure 3(a), providing more insights of the film–substrate relation. The fast Fourier transform diffraction patterns of the MoO_2 film and muscovite are shown in the insets. A clear and sharp interface is observed between the MoO_2 3D structure and the muscovite 2D layered structure. The d-spacing of MoO_2 (002) ($\sim$2.45 Å) is similar to the bulk and is maintained from the interface to the film surface, indicating that there is nearly no strain in the film. Figure 3(d) shows a HR-TEM image exactly at the interface (the marked area) in Figure 3(c). A defect-free and non-coherent interface is observed, showing the presence of a weak interaction between two materials as expected for this system. The TEM, RHEED, and XRD measurements confirm van der Waals epitaxy in the MoO_2/muscovite heterostructures.

After establishing van der Waals epitaxy in the MoO_2/muscovite heterostructure, it is crucial to characterize the functionalities of this system. Since bulk MoO_2 shows metallic behavior, we carried out electrical transport measurements for the MoO_2/muscovite heterostructures. The electrical contacts were fabricated in the van der Pauw configuration. The resistivity as a function of temperature (ρ-T) of the MoO_2 film on muscovite is shown in Figure 4(a). The MoO_2 films are highly conducting ($\rho < 7 \times 10^{-4}$ Ω cm) at room temperature (300 K) and the resistivity decreases with temperature across the entire temperature range, exhibiting nearly metallic behavior. The ρ-T results are in agreement with previous studies of MoO_2 films on the conventional substrates.[39] We also performed temperature dependent Hall measurements to characterize the charge carrier type and carrier concentration of the MoO_2 films. Figure 4(b) shows a typical result of the vertical resistance R_{xy} versus magnetic field, in the range from -2 T to 2 T at 10 K. The positive slope indicates that the charge carriers in MoO_2 are p-type. The carrier concentration given by the inverse relation of the measured Hall coefficient can be extracted as shown in Figure 4(b). The carrier concentration, n, reaches a value of 1.9×10^{22} cm^{-3}, which is much higher than that of other metal oxides. In addition, the carrier concentration in our MoO_2/muscovite systems shows almost no temperature dependence. The calculated mobility of MoO_2 is 0.53 cm^2 V^{-1} s^{-1} at 300 K and 0.97 cm^2 V^{-1} s^{-1} at 2 K, shown in Figure 4(c). Recently, several studies pointed out the existence of ferromagnetism in MoO_2 thin films due to oxygen vacancies.[40] Because the deposition of our films was carried in high vacuum, it is interesting to explore the magnetic properties of the MoO_2 film on muscovite. Therefore, we performed the resistance measurements at 2 K under applied magnetic fields. As shown in Figure 4(d), no obvious magnetoresistance and magnetic hysteresis was

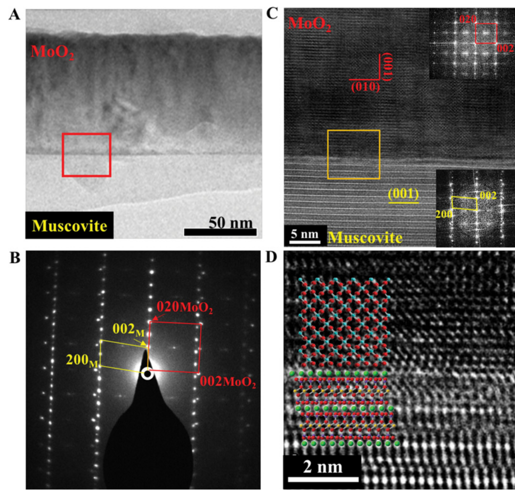

FIG. 3. (a) Cross-sectional TEM image of MoO_2 on muscovite. (b) Electron diffraction pattern at the interface between MoO_2 and muscovite. (c) HR-TEM cross-sectional image at the interface indicated by a red outline in (a) and the corresponding FFT patterns in the inset. (d) Enlarged TEM images taken from the area indicated by yellow square in (c).

observed. A small positive magnetoresistance (1%) was found as expected for conventional metal-like materials. We have also applied the surface-sensitive techniques, X-ray absorption and magnetic circular dichroism (XMCD), to detect magnetic signal with element sensitivity. Negligible XMCD at both Mo L-edge and oxygen K-edge was observed. The superexchange interaction between Mo^{4+} 4d electrons should be mediated by oxygen ions; however, the exchange interaction energy is quite small for 4d electrons, which suggests a very low transition temperature. Therefore, we concluded that the epitaxial MoO_2 thin films on muscovite are non-magnetic at 300 K. The difference in magnetic behaviors between our samples and previous studies could be attributed to the defect mediated magnetism,[41] which is very sensitive to the details of the synthesis process. Based on our results, we concluded that MoO_2/muscovite heterostructure can serve as a bottom electrode or buffer layer to integrate functional oxides into flexible oxide electronics.

We now focus on the benefits of muscovite substrate like being transparent, removable, and flexible. Unlike traditional oxide substrate, mica opens an era for the field of flexible electronics employing epitaxial oxide thin films. In Figure 5(a), we show that our sample is flexible and the sample can be bent without any observable cracks appearing in the system. The sample is semi-transparent because of the deposition of metallic MoO_2 thin film. Due to the weak interaction between layers of muscovite, it can be cleaved much thinner than the traditional oxide substrates, as shown in Figure 5(b). It is possible to remove the entire substrate and to make a free-standing MoO_2 thin film. To explore the electrical behavior of the heterostructures when it is bent, we studied the electrical transport properties as a function of the bending radius at room temperature (300 K). The resistance of the MoO_2 film on muscovite under different bending conditions is shown in Figure 5(c). The resistance remains constant regardless of the bending radius. Because the thickness of the film is very thin (<300 nm) as compared with the bending radius, the strain of the film is too small to affect the conduction. In order to confirm the robust functionalities of MoO_2/muscovite, we have repeatedly bent (more than 500 cycles) the heterostructures to a bending radius of 1 cm, which meets the basic requirements for practical applications. The impact of repeated bending is shown in Figure 5(d). The change in resistance during 500 bending cycles is smaller than 5%, which indicates that this heterostructure is stable after multiple bending cycles. These results suggest that van der Waals epitaxy of functional oxides on muscovite provides a marvelous direction to design and engineer transparent and flexible electronics for practical applications. Moreover, since muscovite can also be used at high temperature (>300 °C), the combination of functional oxides with muscovite will promote high temperature electronics for applications in extreme environments.

To summarize, oxide heteroepitaxy combining 3D functional oxides and 2D layered oxides provides a powerful and nearly universal approach to fabricate flexible or free-standing

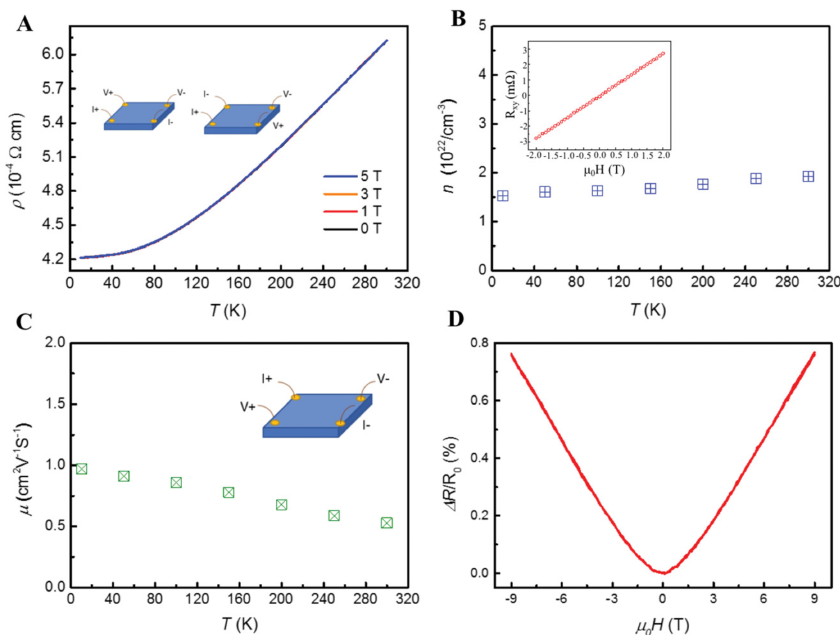

FIG. 4. (a) R-T curve of MoO_2/muscovite and the van der Pauw configuration of the measurement, with the MoO_2 film showing a metallic behavior. (b) Carrier concentration of MoO_2 obtained from Hall measurements. The inset in (b) and (c) show the results and set up of the Hall measurement, respectively. (c) Mobility in the MoO_2 films do not show any obvious temperature dependence. (d) Magnetoresistance measurements at 2 K.

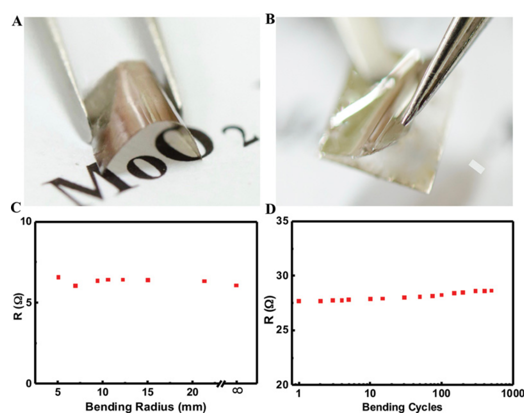

FIG. 5. (a) The flexibility of MoO_2/muscovite sample. (b) Removal of MoO_2 film from muscovite substrate. (c) Resistance of MoO_2/muscovite for different bending radii. (d) Change in resistance during multiple bending cycles.

functional oxide thin films through van der Waals epitaxy. In this study, flexible and transparent muscovite has been used as the substrate for the growth of epitaxial MoO_2 films via PLD. The heteroepitaxy has been confirmed by a combination of RHEED and XRD measurements. A non-coherent and very sharp interface was revealed by TEM, confirming van der Waal epitaxy. Due to the van der Waals bonds between MoO_2 and muscovite, flexible or free-standing MoO_2 films can be fabricated. Furthermore, the same electrical transport behavior observed under various bending conditions confirmed the robust functionalities of the MoO_2 thin films on muscovite. Our study opens an exciting avenue to integrate functional oxides for flexible and transparent electronics.

This work is supported by the Ministry of Science and Technology of Republic of China (under Contract No. MOST 103-2119-M-009-003-MY3), Ministry of Education (Grant No. MOE-ATU 101W961), and Center for Interdisciplinary Science at National Chiao Tung University. The work in University of Science and Technology Beijing is supported by the National Natural Science Foundation of China with Grant Nos. 51371031 and 50971015.

[1] G. Gustafsson, Y. Cao, G. M. Treacy, F. Klavetter, N. Colaneri, and A. J. Heeger, Nature **357**, 477–479 (1992).
[2] R. J. Hamers, Nature **412**, 489–490 (2001).
[3] B. Radisavljevic, M. B. Whitwick, and A. Kis, ACS Nano **5**(12), 9934–9938 (2011).
[4] G. Eda, G. Fanchini, and M. Chhowalla, Nat. Nanotechnol. **3**, 270–274 (2008).
[5] Y. Zhu, S. Murali, W. Cai, X. Li, J. W. Suk, J. R. Potts, and R. S. Ruoff, Adv. Mater. **22**(46), 5226 (2010).
[6] Y. Xu, H. Bai, G. Lu, C. Li, and G. Shi, J. Am. Chem. Soc. **130**(18), 5856–5857 (2008).
[7] K. S. Novoselov, V. I. Fal'ko, L. Colombo, P. R. Gellert, M. G. Schwab, and K. Kim, Nature **490**, 192–200 (2012).
[8] A. K. Geim and K. S. Novoselov, Nat. Mater. **6**, 183–191 (2007).
[9] B. Radisavljevic, A. Radenovic, J. Brivio, V. Giacometti, and A. Kis, Nat. Nanotechnol. **6**, 147–150 (2011).
[10] K. S. Novoselov, A. K. Geim, S. V. Morozow, D. Jiang, Y. Zhang, S. V. Dubonos, I. V. Grigorieva, and A. A. Firsov, Science **306**(5696), 666–669 (2004).
[11] K. S. Novoselov, A. K. Geim, S. V. Morozow, D. Jiang, M. I. Katsnelson, I. V. Grigorieva, S. V. Dubonos, and A. A. Firsov, Nature **438**, 197–200 (2005).
[12] A. H. Castro Neto, F. Guinea, N. M. R. Peres, K. S. Novoselov, and A. K. Geim, Rev. Mod. Phys. **81**, 109 (2009).
[13] K. S. Kim, Y. Zhao, H. Jang, S. Y. Lee, J. M. Kim, K. S. Kim, J.-H. Ahn, P. Kim, J.-Y. Choi, and B. H. Hong, Nature **457**, 706–710 (2009).
[14] S. Bae, H. Kim, Y. Lee, X. Xu, J.-S. Park, Y. Zheng, J. Balakrishnan, T. Lei, H. R. Kim, Y. I. Song, Y.-J. Kim, K. S. Kim, B. Özyilmaz, J.-H. Ahn, B. H. Hong, and S. Iijima, Nat. Nanotechnol. **5**, 574–578 (2010).
[15] X. Li, Y. Zhu, W. Cai, M. Borysiak, B. Han, D. Chen, R. D. Piner, L. Colombo, and R. S. Ruoff, Nano Lett. **9**(12), 4359–4363 (2009).
[16] M. Xu, T. Liang, M. Shi, and H. Chen, Chem. Rev. **113**(5), 3766–3798 (2013).
[17] S. Z. Butler, S. M. Hollen, L. Cao, Y. Cui, J. A. Gupta, H. R. Gutiérrez, T. F. Heinz, S. S. Hong, J. Huang, A. F. Ismach, E. Johnston-Halperin, M. Kuno, V. V. Plashnitsa, R. D. Robinson, R. S. Ruoff, S. Salahuddin, J. Shan, L. Shi, M. G. Spencer, M. Terrones, W. Windl, E. Joshua, and J. E. Goldberger, ACS Nano **7**(4), 2898–2926 (2013).
[18] Q. H. Wang, K. Kalantar-Zadeh, A. Kis, J. N. Coleman, and M. S. Strano, Nat. Nanotechnol. **7**, 699–712 (2012).
[19] A. K. Geim and I. V. Grigorieva, Nature **499**, 419–425 (2013).
[20] D. Jariwala, V. K. Sangwan, L. J. Lauhon, T. J. Marks, and M. C. Hersam, ACS Nano **8**(2), 1102–1120 (2014).
[21] H. Y. Hwang, Y. Iwasa, M. Kawasaki, B. Keimer, N. Nagaosa, and Y. Tokura, Nat. Mater. **11**, 103–113 (2012).
[22] J. Mannhart and D. G. Schlom, Science **327**(5973), 1607–1611 (2010).
[23] H. Takagi and H. Y. Hwang, Science **327**(5973), 1601–1602 (2010).
[24] A. Koma, Thin Solid Films **216**(1), 72–76 (1992).
[25] A. Koma, J. Cryst. Growth **201–202**, 236–241 (1999).
[26] M. I. B. Utama, Q. Zhang, J. Zhang, Y. Yuan, F. Belarre, J. Arbiol, and Q. Xiong, Nanoscale **5**, 3570–3588 (2013).
[27] W. Yang, G. G. Chen, Z. Shi, C.-C. Liu, L. Zhang, G. Xie, M. Cheng, D. Wang, R. Yang, D. Shi, K. Watanabe, T. Taniguchi, Y. Yao, Y. Zhang, and G. G. Zhang, Nat. Mater. **12**, 792–797 (2013).
[28] J.-H. Lee, E. K. Lee, W.-J. Joo, Y. Jang, B.-S. Kim, J. Y. Lim, S.-H. Choi, S. J. Ahn, J. R. Ahn, M.-H. Park, C.-W. Yang, B. L. Choi, S.-W. Hwang, and D. Whang, Science **344**(6181), 286 (2014).
[29] D. Dumcenco, D. Ovchinnikov, K. Marinov, P. Lazić, M. Gibertini, N. Marzari, O. L. Sanchez, Y.-C. Kung, D. Krasnozhon, M.-W. Chen, S. Bertolazzi, P. Gillet, A. F. i Morral, A. Radenovic, and A. Kis, ACS Nano **9**(4), 4611–4620 (2015).
[30] J. Kim, C. Bayram, H. Park, C.-W. Cheng, C. Dimitrakopoulos, J. A. Ott, K. B. Reuter, S. W. Bedell, and D. K. Sadana, Nat. Commun. **5**, 4836 (2014).
[31] Y. J. Hong and T. Fukui, ACS Nano **5**(9), 7576–7584 (2011).
[32] M. I. B. Utama, Q. Zhang, S. Jia, D. Li, J. Wang, and Q. Xiong, ACS Nano **6**(3), 2281–2288 (2012).
[33] M. I. B. Utama, F. J. Belarre, C. Magen, B. Peng, J. Arbiol, and Q. Xiong, Nano Lett. **12**(4), 2146–2152 (2012).
[34] P. K. Mohseni, A. Behnam, J. D. Wood, C. D. English, J. W. Lyding, E. Pop, and X. Li, Nano Lett. **13**(3), 1153–1161 (2013).
[35] J. A. DeRose, T. Thundat, L. A. Nagahara, and S. M. Lindsay, Surf. Sci. **256**(1–2), 102–108 (1991).
[36] S. Song, W. S. Kim, J. M. Ha, G. G. Lee, J.-H. Ku, H. S. Kim, C. S. Kim, C. J. Choi, T. H. Choe, J. Y. Yoo, W. S. Song, J. W. Park, S. H. Jeong, D. H. Baek, K. Fujihara, H. K. Kang, S. I. Lee, and M. Y. Lee, IEDM Tech. Dig. **1999**, 427–430.
[37] E. M. Kaidashev, M. Lorenz, H. von Wenckstern, A. Rahm, H.-C. Semmelhack, K.-H. Han, G. Benndorf, C. Bundesmann, H. Hochmuth, and M. Grundmann, Appl. Phys. Lett. **82**, 3901 (2003).
[38] C. Simbrunner, G. Hernandez-Sosa, M. Oehzelt, T. Djuric, I. Salzmann, M. Brinkmann, G. Schwabegger, I. Watzinger, H. Sitter, and R. Resel, Phys. Rev. B **83**, 115443 (2011).
[39] V. Bhosle, A. Tiwari, and J. Narayan, J. Appl. Phys. **97**, 083539 (2005).
[40] P. Thakur, J. C. Cezar, N. B. Brookes, R. J. Choudhary, R. Prakash, D. M. Phase, K. H. Chae, and R. Kumar, Appl. Phys. Lett. **94**, 062501 (2009).
[41] J. Li, S. Zhang, J. Bartell, C. Nisoli, X. Ke, P. E. Lammert, V. H. Crespi, and P. Schiffer, Phys. Rev. B **82**, 134407 (2010).